

Numerical characterization under uncertainties of a piston expander for exhaust heat recovery on heavy commercial vehicles

P.M. Congedo¹, J. Melis², R. Daccord²

¹ INRIA Bordeaux Sud-Ouest, 200 Rue de la Vieille Tour, 33405 Talence, France

² EXOES, 6 Avenue de la Grande Lande, 33170 Gradignan, France

E-mail: pietro.congedo@inria.fr, julien.melis@exoes.com, remi.daccord@exoes.com

Abstract. While nearly 30 percent of the fuel energy is lost as waste heat in the form of hot exhaust gases, exhaust heat recovery promises one of the biggest fuel economy potential regarding the technologies available in the next decade. Applied to heavy commercial vehicles (HCVs), buses or off road vehicles, a bottoming Rankine Cycle (RC) on exhaust heat shows a great potential in recovering the exhaust gases energy, even for part loads. The objective of this paper is to illustrate the interest in assessing the uncertainty of this kind of systems for getting a robust prediction of the associated numerical model. In particular, the focus here is on the simulation of a piston expander for exhaust heat recovery.

Uncertainties associated to the experimental measurements are propagated through the numerical code by means of uncertainty quantification techniques. Several sources of uncertainties are taken into account at the same time, thus yielding various indications concerning the most predominant parameters, and their influence on several quantities of interest, such as the mechanical power, the mass flow and the exhaust temperature.

1. Introduction

To date, emission regulations focusing on local pollutants have limited the potential efficiency gains of internal combustion engine (ICE). However, future regulations will focus on CO₂ emissions, requiring high efficiency increase of the whole drivetrain. The best efficiency of a modern ICE will remain below 42%. Electrification of ancillaries and hybridization seem to lead to little fuel cuts on Heavy Commercial Vehicles (HCVs) and, at least, would be too expensive to reach future CO₂ emissions regulation compared to air drag reduction and waste heat recovery (WHR). While HCVs aerodynamic is mostly constrained by regulation and also depends on trailer manufacturers, WHR appears as essential in the future innovation panel for HCVs. Though the potential of WHR is clear, the technology has to prove the business, durability and safety cases to be launched in mass production.

A great interest has been developed in the last years concerning the potential new technologies for exploiting the waste heat recovery (WHR) from IC engines. Several options have been investigated [1]: Organic Rankine Cycles [2], six-stroke cycle IC engine [3], thermoelectric generator [4], turbocharger technology [5, 6]. Among several technologies, Rankine cycles (RC) seem promising to win the competition regarding their efficiency, cost and maturity. The key



components of a RC are shown hereafter (see Figure 1). Key choices when designing such a system are the selection of the hot source, the working fluid, the expander and the cold sink.

ORC technology for recover low grade heat sources, such as in solar or geothermal plant, feature the use of turbines, scroll expander, screw expander [7]. Nevertheless, these solutions are not ideal when considering the WHR in IC engines because of the space and weight constraints. For this reason, some studies are focused on the development of an ORC design presenting a reciprocating machine, permitting an optimal recovery of the waste heat energy, based on a low working fluid flow, high values in expansion ratios and space restrictions. Some works [8] have been devoted to the design of an ORC facility for waste heat recovery in IC engines. Several studies [9, 10, 11, 13, 14, 15] suggested the use of a piston expander for exhaust heat recovery (EHR). In [12], they tested an axial piston expander and calibrated a semi-empirical model.

Uncertainty quantification (UQ) is an emerging field in scientific computing. UQ methods compute the impact of inevitable uncertainties in boundary and initial conditions, and in model parameter inputs on the output quantities of interest. One of the objectives of UQ is to enable a more rigorous comparison between numerical predictions and experimental measurements with their respective uncertainty margins. Few works exist on the application of these techniques in ORC-based framework (see for example [17, 18, 19]).

In this paper, we focus on a piston expander (designed by the Exoès engineering company) devoted to exhaust heat recovery, and how uncertainty quantification techniques could be exploited in order to characterize the global performances of the system and to drive further improvements. After providing a general description of the expander in Section 2, the numerical model and an analysis over the main uncertainties of the system are presented in Section 3. Some results are provided in Section 4, and conclusions are drawn in Section 5.

2. Description of the expander

While using a RC, the majority of the tailpipe exhaust heat will be rejected in the cooling fluid under hood. A trade-off due to weight, packaging, fan engagement and aero complexities must be found. Designing a compact cooling system is also a main challenge to reach the expected fuel consumption reduction [16]. Exoès decided to use the existing ICE cooling loop to avoid an additional front radiator and to be compatible with all the different truck cooling architectures. Exoès assume then a cooling temperature between 75 and 95°C according to a typical front radiator management of a HCV.

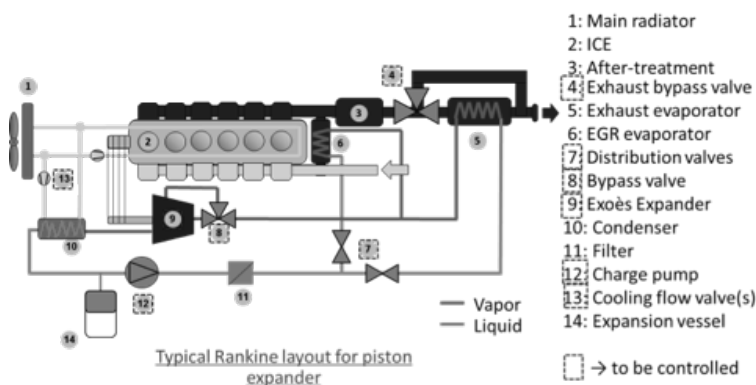


Figure 1. Bottoming cycle on exhaust line.

As we focus on the expander, what matters are the expander boundaries: the connections to the RC with vapor state points and the connection to the ICE with its speed. These boundaries are summed up in table 1. The main performance objectives for this prototype are summed up in table 2.

Table 1. Expander boundaries.

	Nominal ranges	Design Point	Full Load
Inlet pressure [Bar]	10-35	20	35
Inlet temperature [°C]	180-240	210	240
Outlet pressure [Bar]	1-2.3	1.2	2.3
Engine Speed [Rpm]	600-1800	1200	1200
Massflow [g/s]	20-80	40	80

Table 2. Expander performance target (The maximal effective isentropic efficiency is obtained at an outlet pressure of 1.2 Bar).

	Target	Achieved to date
Max effective isentropic efficiency	>60%	54%
Weight (without the coupling to the ICE)	12	18
Size (without the coupling to the ICE)	D180xL300	D215xL350

The expander is built on three double acting crosshead pistons arranged around a swash plate (see Figure 2). The machine has been designed to be mechanically coupled to an ICE on the front end accessory drive with a pulley, or on the back of the ICE through the gear of a power-take-off. The expander can be declutched or not. This feature may be granted by a free wheel, a clutch or a gearbox. The inlet system has been developed and patented to work at 250°C and to endure the heavy accelerations required to supply this two-stroke high speed steam engine. Together with the piston rings, the poppet valves of the inlet system also work with the scarce lubrication provided by the circulating oil not viscous enough at these high temperatures. The lubrication of the expander is controlled through an internal oil pump directly mounted on the shaft tip. The oil is pumped in the oil tank at the bottom of the expander. The oil passes through an oil filter integrated in the expander and is ducted through the shaft and/or through the crankcase to distribute lubricant in the swashplate chamber including the bearings, in the inlet valves chambers and on the shaft seal. An integrated oil separator at the outlet port recovers the possible leaks of oil into the vapor to fill them back to the tank.

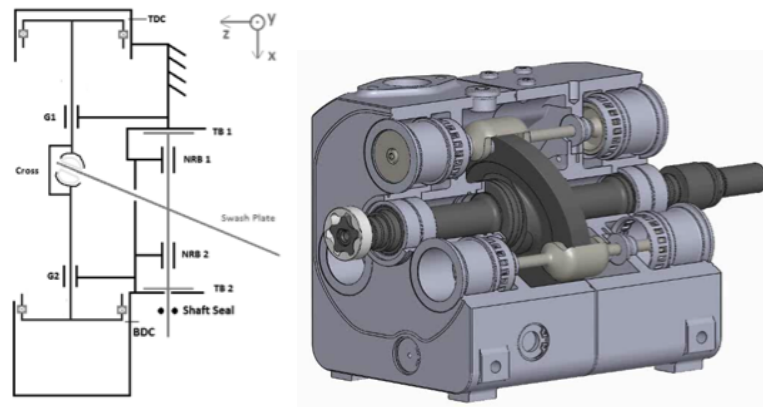


Figure 2. Expander architecture.

3. Numerical model

A Matlab 1D expander model has been built. The model consists in calculating the in-cylinder pressure during a complete rotation and ensuring the convergence of the computed mass-flow.

The model carries out the balances of energy and mass in the inlet and outlet collectors as well as in the piston chamber discretized per each half shaft angle of rotation (denoted with a subscript i in the scheme reported in Figure 3). Note that the software Refprop [20] is used to compute the thermodynamic behavior of the working fluid. In addition, several losses are taken into account as described in the scheme presented in Figure 3. As a result, a typical Pressure-Volume diagram is computed (see Figure 4) as well as all the macroscopic values, such as massflow (\dot{M}), mechanical power (\dot{W}), exhaust temperature (T_{out}) :

$$(\dot{M}, \dot{W}, T_{out}) = f(RPM, P_{in}, h_{in}, P_{out}, X_j) \quad (1)$$

where P_{in} and h_{in} are the inlet pressure and enthalpy, P_{out} is the outlet pressure, and X_j are some parameters calibrated with respect to the experimental data.

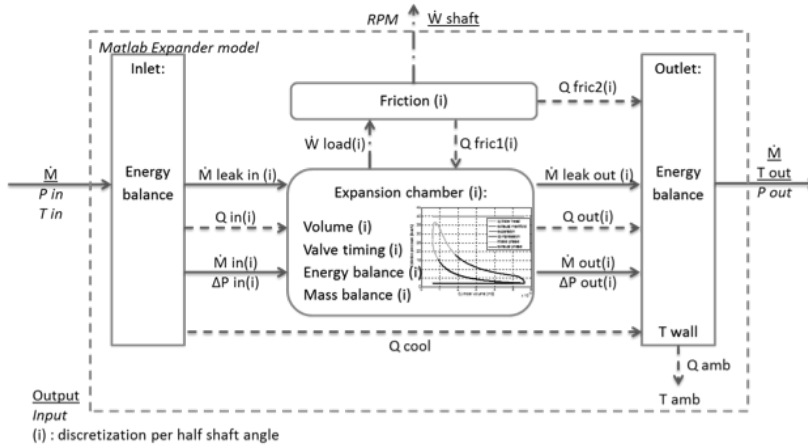


Figure 3. Expander model.

The model f is formulated according to the following hypothesis :

- The pressure losses during the intake and the exhaust phases are calculated through a calibrated discharge coefficient applied to theoretical flow crossing the throat.
- The steam properties and velocity at the throat are computed assuming that the flow is isentropic before the throat and isenthalpic on the total transformation.
- Leaks are modeled through the piston rings, the inlet valve seat and the inlet valve guide with Couette-Poiseuille equations.
- Convective heat transfers is implemented with a fixed convective heat transfer coefficient that has to be calibrated. Heat transfer occurs between inlet and outlet, inlet and cylinder chamber, cylinder chamber and outlet and through cylinder walls.
- Friction models use a simple calibrated friction coefficient, except for the sliding shoe on the plate. For this contact a dedicated 2D model is used to calculate the oil film thickness and then the equivalent friction coefficient.

The working fluid is a mixture constituted by water 4.4%wg, ethanol 92.6%wg and lubricant 3%wg. For calculations hereafter we simplify the mixture neglecting the lubricant percentage.

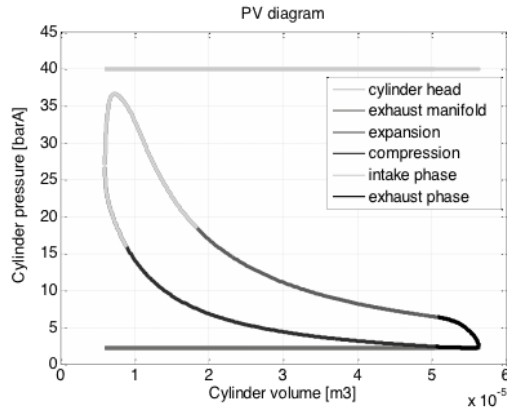


Figure 4. PV diagram.

3.1. Uncertainty assessment and design variables

We have identified three different sets of parameters. First group is related to some physical parameters, which are characterized in terms of uncertainties, but they are not treated as design variables. In practice, only certain nominal conditions are taken into account, without exploring the design space. These variables are the following : Cylinder Head Enthalpy, Bore, Stroke, Implantation radius, Inlet diameter, Outlet width, Half ball radius.

Second group is related to the parameters which are characterized in terms of uncertainties and also their variability in a larger design space is explored. These parameters are the Rotational speed, Cylinder Head Pressure, Exhaust pressure, Dead volume, Inlet lift, Outlet lift.

The third group of parameters is associated to the set of calibration parameters. In this case, since these parameters have been obtained by performing a calibration starting from experimental data, it is harder to fully characterize their variability. For this reason, concerning the uncertainty on calibration parameters, we consider a ± 0.01 variation based on some experimental evidence [14], which should provide a first estimation about the potential influence of the uncertainty on these parameters. Future studies should consider a larger variation, or solving the whole problem by means of Bayesian-based approaches. Finally, the following calibration parameters are considered: Inlet Leak coefficient (denoted with X1 in the following), Piston Leak coefficient (X2), Inlet Silent coefficient (X3), Outlet Silent coefficient (X5), Intern heat transfer coefficients (X6), Extern heat transfer coefficients (X7), Dead Volume coefficient (X8), Inlet Lash coefficient (X9), Discharge coefficient (X10), Relative Pressure coefficient (X13), PS Friction Coefficient (X14), SSP Friction Coefficient (X15).

The variation of the whole set of parameters are then resumed in Figure 3.

3.2. Numerical method for uncertainty quantification

Let us consider a stochastic differential equation of the form:

$$L(\mathbf{x}, \boldsymbol{\xi}, \phi) = f(\mathbf{x}, \boldsymbol{\xi}) \quad (2)$$

where L is a non-linear spatial differential operator (for instance, L is the steady Navier-Stokes operator) depending on a set of uncertainties, defined with a random vector $\boldsymbol{\xi}$ (whose dimension depends on the number of uncertain parameters in the problem) and $f(\mathbf{x}, \boldsymbol{\xi})$ is a source term depending on the position vector \mathbf{x} and on $\boldsymbol{\xi}$. The solution of the stochastic equation (2) is the unknown dependent variable $\phi(\mathbf{x}, \boldsymbol{\xi})$, and is a function of the space variable $\mathbf{x} \in \mathbf{R}^d$ and of $\boldsymbol{\xi}$. One of the objective of Uncertainty Quantification is to compute the statistics of the quantity of interest, *i.e.* $\phi(\mathbf{x}, \boldsymbol{\xi})$ with respect to the system uncertainties $\boldsymbol{\xi}$.

Table 3. Uncertainty assessment.

Parameter	Nominal Point	Uncertainty
Rotational Speed (tr/min)	3000	0.30%
Cylinder Head Pressure (barA)	25	0.36 bar
Cylinder Head Temperature (°C)	210	5°C
Cylinder Head Enthalpy (kJ/Kg)	1094.27	1.30%
Exhaust pressure (barA)	1.3	0.06bar
Bore (mm)	40	0.12mm
Stroke (mm)	40.04	0.10%
Implantation radius (mm)	55	0.40%
Dead volume (cc)	6.13	6.0%
Inlet diameter (mm)	10	0.40%
Inlet lift (mm)	2	0.05mm%
Inlet duration (°)	82	2°
Inlet top angle (° after TDC)	15.5	2°
Outlet lift (mm)	4.5	0.33mm
Outlet width (%)	65	0.30%
Inlet leak coefficient (X1)	0.036	0.01
Piston leak coefficient (X2)	1.94	0.01
Inlet silent coefficient (X3)	0.1	0.01
Outlet silent coefficient (X4)	0.0	0.01
Inlet heat transfer coefficient (X5)	2.22	0.01
External heat transfer coefficient (X6)	1.62	0.01
Inlet valve stem leak coefficient (X7)	0.969	0.01
Dead volume coefficient (X8)	1.03	0.01
Inlet lash coefficient (X9)	0.978	0.01
Discharge coefficient (X10)	1.36	0.01
Relative pressure coefficient (X13)	0.911	0.01
PS friction coefficient (X14)	0.145	0.01
SSP friction coefficient (X15)	0.235	0.01

Using a non-intrusive uncertainty quantification tool means that a single deterministic computation (used to solve for example the differential operator L) is replaced with a whole set of such computations, each one of those being run for specific values of the uncertain conditions. In this work, a non-intrusive techniques is used to propagate physical uncertainties through the system under consideration. An anchored-ANOVA [21, 22] approach is applied in this paper, since a large set of uncertainties is analyzed here (the method can treat until hundreds of uncertainties). This analysis permits to detect the hierarchy of the most predominant uncertainties and sensibly reduced the number of deterministic simulations needed to perform the stochastic analysis.

4. Results

This section is devoted to present the results coming from different sensitivity analysis, which are performed considering several sets of conditions. Note that the sensitivity analysis is performed for each of the four quantities of interest in this study: the mechanical power, the mass flow rate, the exhaust temperature and the isentropic efficiency, defined as $\Delta h / \Delta h_{ideal}$ where Δh

represents the variation of the static enthalpy between inlet and outlet boundaries, and Δh_{ideal} is the variation of enthalpy when an ideal isentropic transformation with the same initial conditions and pressure ratio as the real flow.

First, the uncertainties on the physical parameters are taken into account, then a problem with 14 (fourteen) uncertainties should be solved. Secondly, the sensitivity analysis is extended by including also the uncertainties coming from the calibration parameters. The interest is into a deeper understanding of the most predominant set of parameters. In this case, a problem with 26 (twenty-six) parameters has to be treated.

Let us present the result coming from the sensitivity analysis applied to the problem featuring 14 (fourteen) uncertainties on the physical parameter. First, a sensitivity analysis study is applied to the variability of the Mechanical Power, which has been reported in Figure 5. As it can be easily observed, there are three predominant uncertainties (Dead volume, rotational speed, exhaust pressure, in order of importance), and a fourth (inlet lift) with a small contribution. Concerning the variability associated to the Mass flow rate, plotted in Figure 6, the uncertainty on the Dead Volume contributes nearly to the 60% of the variance. Three other uncertainties, *i.e.* on the cylinder head pressure, on the cylinder head enthalpy and on the exhaust pressure contribute nearly to the 36% of the variance. Note also that another uncertainty, *i.e.* on the inlet lift, contribute nearly to the 2%, while all the other uncertainties can be neglected. Finally, the results of the sensitivity analysis is reported in Figure 7 for the exhaust temperature and in Figure 8 for the isentropic efficiency, respectively. Concerning the variability of the exhaust temperature, the uncertainty on the cylinder head enthalpy contributes the most, attaining nearly the 97% of the total variance. Concerning the isentropic efficiency, there are two predominant uncertainties, on the exhaust pressure and on the dead volume, which contribute nearly to the 90% of the variance.

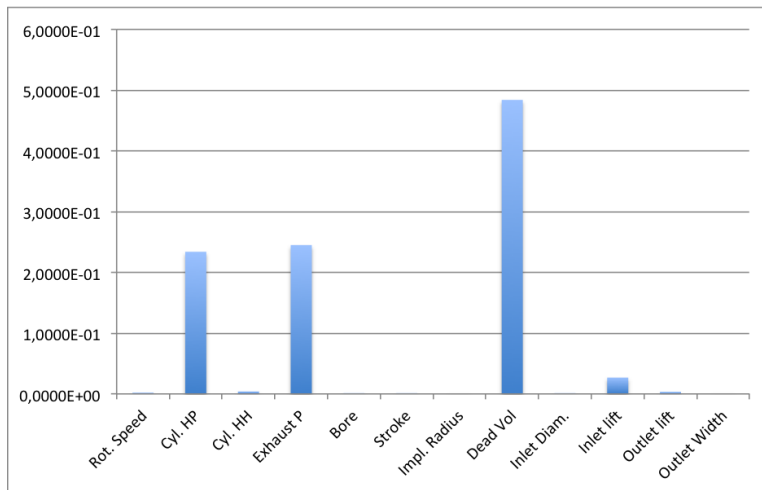


Figure 5. Hierarchy of the most predominant parameters for the Mechanical Power.

Let us now introduce the results of the sensitivity study when also the uncertainties on the calibration parameters are introduced. Note that in this case, a fixed variation interval has been imposed for each uncertainty. Results for the mechanical power (only this figure is reported in this paper, *i.e.* Figure 9, for sake of brevity), mass flow, exhaust pressure and isentropic efficiency, show that the hierarchy computed by considering only the uncertainties on the physical parameters remains nearly the same for each quantity of interest. Then, the influence of the calibration parameter can generally be considered as negligible with respect to the uncertainty of the physical parameters. Note then that the only parameter that provides a certain contribution to the global variance is the Dead volume coefficient, attaining nearly the 1%, in the context of the sensitivity analysis for the mechanical power, the mass flow, and the

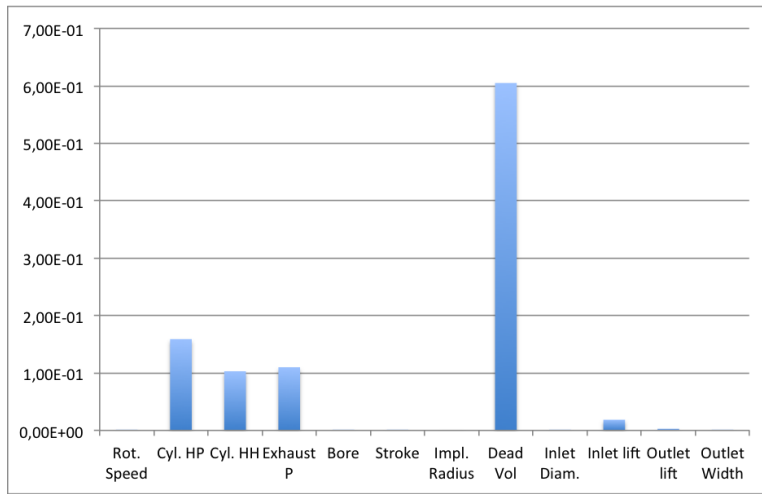


Figure 6. Hierarchy of the most predominant parameters for the Mass Flow.

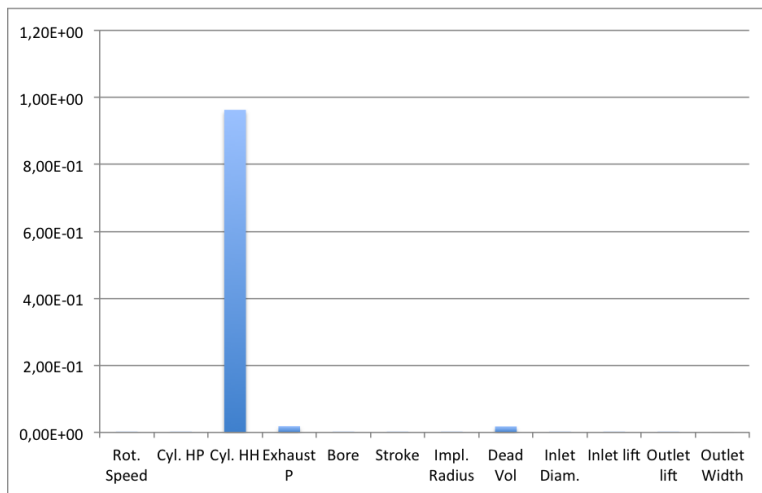


Figure 7. Hierarchy of the most predominant parameters for the Exhaust Temperature.

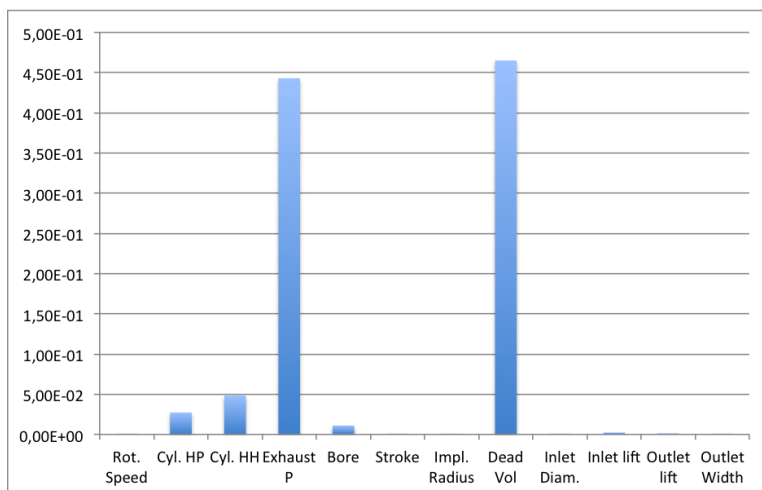


Figure 8. Hierarchy of the most predominant parameters for the Isentropic efficiency.

isentropic efficiency.

Note that anyway this analysis could be in theory biased by the assumption about the interval variation, which has been imposed to each calibration parameter, in absence of a more

Table 4. Some statistics for the Mechanical Power, the Mass Flow, the exhaust temperature, and the isentropic efficiency.

	Mech. Pow. [kW]	Massflow [kg/s]	Exh. Temp. [°C]	Net Is. Eff. [%]
μ	8.541781	67.29476	100.6077	61.36836
σ	0.05593562	0.5739631	1.584921	0.07429255
COV	0.006548473	0.00852909	0.01575348	0.0012106
90% conf. interv.	(8.4510 ; 8.6362)	(66.473 ; 68.321)	(98.289 ; 103.265)	(61.220 ; 61.463)

precise characterization. Clearly, if the interval variation is increased, the expected behavior could feature also an increasing importance of the uncertainty on the calibration parameter. Nevertheless, this study provides an useful indication about the non-influence of these parameters when a reduced interval variation is considered. An optimal way to further investigate this problem could be the calibration of these parameters by means of a bayesian approach starting directly from the experimental data.

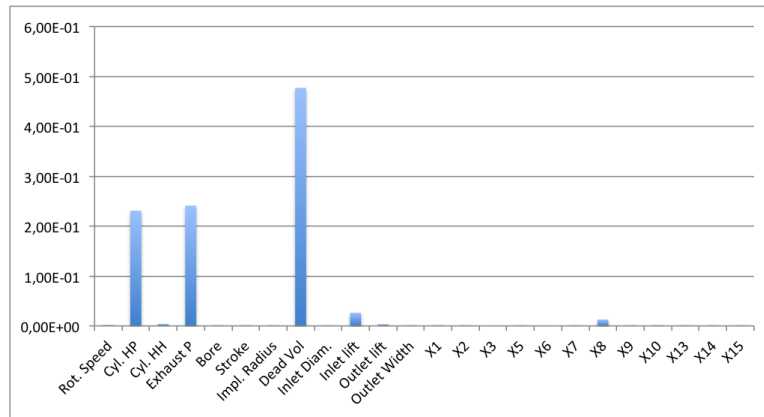


Figure 9. Hierarchy of the most predominant parameters for the Mechanical Power, considering the uncertainties both on the physical and calibration parameters.

Moreover, in Table 4, several statistical quantities are computed, in particular the mean, the standard deviation, the coefficient of variation (standard deviation to mean ration), the 90% confidence interval. Note that the PDF of the mechanical power is truly of gaussian-type (see Figure 10), with a coefficient of variation of 0.6%. The PDF of the exhaust temperature (see Figure 11) displays a quasi multi-modal behavior with two peaks at 99°C and 102°C. In this case, the coefficient of variation is much higher, attaining 1.5%.

5. Conclusions

This paper illustrates a study concerning the uncertainty characterization and assessment of the simulation of a piston expander for waste heat recovery. Experimental and model parameters uncertainties are propagated through a simple numerical model in order to get the sensitivity analysis for some important quantities of interest, such as the mechanical power, the mass flow and the exhaust pressure. Results show that the uncertainty on the dead volume contributes largely to the variance of each quantity of interest except for the exhaust temperature. This last one is mostly dependent on the uncertainty of the cylinder head enthalpy. Other quantities to control (since they explain a large contribution to the variance) are the exhaust pressure and the rotational speed, which affect the variance of the mechanical power and of the isentropic

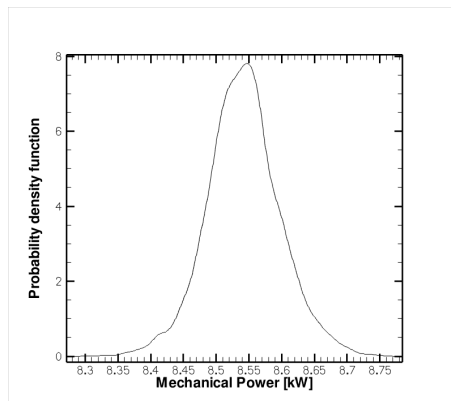


Figure 10. PDF of the mechanical power.

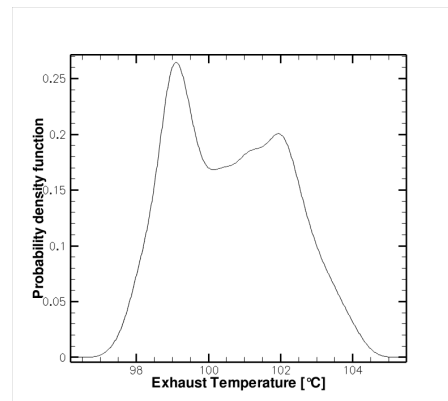


Figure 11. PDF of exhaust temperature.

efficiency as well. On the contrary, uncertainties on the calibration parameters are negligible. Globally, the min/max variation for each quantity of interest is around 3%, then, they are quite stable w.r.t. the system uncertainties.

This analysis has then permitted to identify four important parameters (on twenty-six) to control in order to reduce the global amount of uncertainty associated to the quantity of interest, thus providing interesting insights for the model improvement. Future works should be directed to extend this study including a larger set of operating conditions and to the calibration of the model parameters, exploiting directly the experimental data.

References

- [1] Saidur R and Rezaei M and Muzammil W and Hassan M and Paria S and Hasanuzzaman M 2015 *Renewable and Sustainable Energy Reviews* **16** 1260-1268.
- [2] Apostol V and Pop H and Dobrovicescu A and Prisecaru T and Alexandru A and Prisecaru M 2015 *Procedia Engineering* **100** 549-558.
- [3] Conklin J and Szybist J 2014 *Energy Procedia* **45** 121-130.
- [4] Yang J 2005 *24th International Conference on Thermoelectrics* 1-5.
- [5] Dolz V and Novella R and Garcia A and Sanchez J 2012 *Applied Thermal Engineering* **36** 269-278.
- [6] Serrano J and Dolz V and Novella R and Garcia A 2012 *Applied Thermal Engineering* **36** 279-287.
- [7] Qiu G and Liu H and Riffat S 2011 *Applied Thermal Engineering* **31** 3301-3307.
- [8] Macian V and Serrano J and Dolz V and Sanchez J 2013 *Applied Energy* **104** 758-771.
- [9] Demler R 1976 *SAE Int. Tech. Paper* 1-15.
- [10] Badami M and Mura M 2009 *Energy* **34** 1315-1324.
- [11] Endo T and Kawajiri S and Kojima Y and Takashi K 2007 *SAE World Congress* 1-10.
- [12] Glavatskaya Y and Podevin P and Lemort V and Shonda O and Decombes G 2012 *Energies* **5** 1751-1765.
- [13] Daccord R and Kientz T and Melis J 2013 *ASME ORC 2013*.
- [14] Daccord R and Darmedru A and Melis J 2014 *SAE 2014 World Congress & Exhibition 2014-01-0675* 12.
- [15] Galindo J and Dolz V and Royo L and Haller R and Melis J 2015 *3rd International Seminar on ORC Power Systems* **85** 17.
- [16] Dickson J and Ellis M and Rousseau T 2014 *SAE International*. **2014-01-2339** 99-120.
- [17] Abgrall R and Congedo PM and Geraci G and Iaccarino G 2016 *CMAME*. **301** 80-115.
- [18] Congedo PM and Geraci G and Abgrall R and Pediroda V and Parussini L 2013 *Engineering Computations*. **30** 1032-20153.
- [19] Congedo PM and Corre C and Martinez JM 2011 *CMAME*. **200** 216-232.
- [20] Lemmon EW and Huber ML and McLinden MO 2013 *NIST Standard Reference Database 23: Reference Fluid Thermodynamic and Transport Properties-REFPROP, Version 9.1*. NIST.
- [21] Tang K and Congedo PM and Abgrall R 2015 *IJNME*. **102** 1584.
- [22] Tang K and Congedo PM and Abgrall R 2016 *Journal of Computational Physics*. **314** 589.